Molecular analysis by ionization of laser-desorbed neutral species

Keith R. Lykke, Peter Wurz, Deborah H. Parker, Michael J. Pellin

A powerful molecular surface analysis technique for the analysis of complex materials, such as polymer/additive systems, consists of laser desorption of surface molecules and subsequent ionization of these gas-phase molecules with resonant or nonresonant laser ionization. These molecular ions are subsequently detected by Fourier-transform mass spectrometry or time-of-flight mass spectrometry. We show that different wavelengths for the postionization step permit selectivity that provides important additional information on the chemical makeup of these complex materials. Near-UV wavelengths selectively ionize aromatic polymer additives, far-UV wavelengths photoionize other nonaromatic species; and vacuum-UV wavelengths provide access to all the desorbed species. In addition to these applied results, we study many fundamental issues of laser desorption, such as desorption thresholds, velocity distributions, postionization wavelength selectivity, etc. The Fourier-transform mass spectrometer and time-of-flight mass spectrometer are discussed in detail.

Key words: Molecular surface analysis, mass spectrometry, laser desorption.

1. Introduction

The ability to analyze surface elemental composition has existed for some time. The various methods include Auger electron spectroscopy, x-ray photoelectron spectroscopy, secondary ion mass spectrometry, and the various forms of secondary neutral mass spectrometry.[1] However, molecular surface analysis is only now achieving comparable sensitivity and selectivity. Molecular surface analysis can be achieved by utilizing various optical probes: IR reflection absorption spectroscopy,[2,3] sum-frequency (or second-harmonic) generation spectroscopy on surfaces,[4,5] etc. These techniques are generally lacking species-specific information, particularly when applied to complex surfaces. Another approach is to remove the molecule from the surface and probe it in the gas phase by molecular mass spectrometry (Fig. 1). State-of-the-art mass spectrometry[6–8] offers the high resolution and the high sensitivity that are necessary for these kinds of investigation. The remaining problems for molecular analysis are removal of the molecule from the surface and ionization of the molecule without alteration (i.e., fragmentation). In particular, these processes pose serious complications for large molecules. Furthermore, if the molecule of interest is only a minor constituent of a sample and falls in the same mass range as either the major components or their fragmentation products, mass resolution and sensitivity alone are not sufficient for species identification. Thus a preselection in the ionization process becomes necessary. Our solution is to employ lasers for both desorption from the sample and ionization (postionization) in the gas phase of the neutral desorbed species. The ability to choose both the wavelength and the intensity of the desorption laser as well as the postionization laser permits proper tailoring to the actual needs of the investigation.

In the case of relatively simple systems in which only mass identification is required, mass spectrometry of directly emitted ions may be sufficient. However, for quantitative analysis or selectivity, postionization of desorbed neutral molecules is necessary. Lasers have been exploited for mass removal from surfaces for a number of years. For early work on the subject, consult the book by Ready.[9] Many articles in the book edited by Lubman[10] detail recent mass spectrometric findings. At least two different mechanisms exist for the removal of surface molecules by laser desorption. One involves the thermal evaporation of species by local heating of the irradiated spot. In this process, the laser photons are absorbed in the near-surface region, resulting in local heating and thermal desorption of surface species. The other mechanism involves bond rupture that results from molecular electronic excitation, which is

The authors are with the Materials Science/Chemistry Divisions, Argonne National Laboratory, Argonne, Illinois 60439.

Received 1 July 1992.

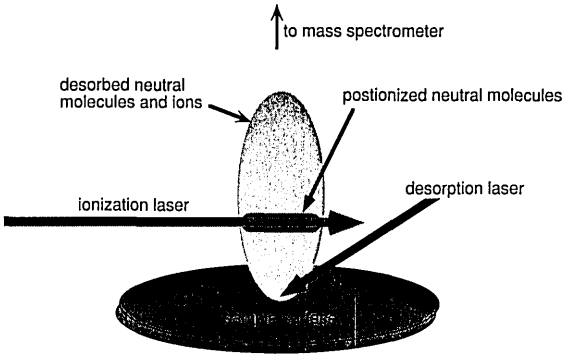

Fig. 1. Illustration of the laser-desorption–laser-ionization event. The desorption plume contains molecular ions and neutrals. The neutral molecules are usually orders of magnitude more abundant than ions. The ionization laser is positioned much closer to the surface than is depicted here to interact with as many desorbed molecules as possible.

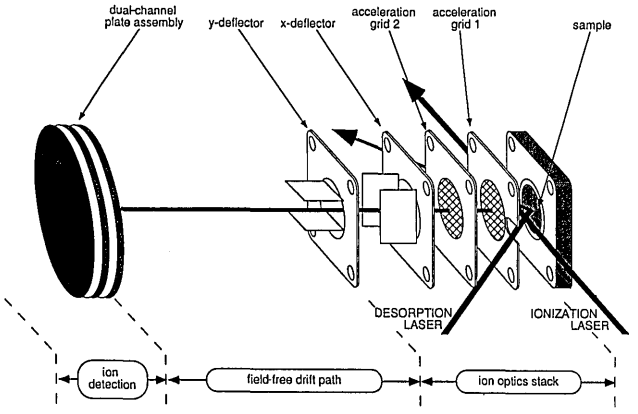

Fig. 2. Schematic of the laser-desorption TOF apparatus. The sample is mounted on a rapid sample transfer rod and loaded into the system, and then the rod is retracted. The sample is typically at 8 kV and grid 1 is at 7.6 kV for postionization or 0 kV for prompt ion detection. The laser beams enter and exit the apparatus through fused-silica windows.

usually observed for far-UV light. This type of process has been referred to as ablative photodecomposition.[11] There have been numerous papers and reviews on each of these phenomena.[12–14] The distinction between these two mechanisms is often vague, and both may occur simultaneously. However, the thermal mechanism seems to explain most of the data in this work.

In this paper we discuss various aspects of laser-desorption mass spectrometry, including desorption thresholds for ions (both positive and negative) and neutral molecules, velocity distributions of the desorbed neutral species, and laser ionization of molecules. The latter is illustrated with a few representative examples of applications of the technique. First, a vulcanizate (rubber) is analyzed with a time-of-flight (TOF) mass spectrometer and a Fourier-transform mass spectrometer (FTMS) for the organic additives present in minor concentrations in the near-surface region. Second, a new class of carbon molecule (fullerenes) is examined with a FTMS. Finally, some recent work on tunable vacuum-UV (VUV) postionization mass spectrometry is presented.

2. Experimental

A. Time-of-Flight Instrument

The laser desorption TOF apparatus (Fig. 2) has been discussed in detail previously.[15,16] The mass spectrometer is established by a sample surface, an acceleration field, and a field-free region with an ion detector at the end of the flight path. The TOF mass spectrometer can be operated in either of two modes. First, for measuring the mass spectrum of laser-desorbed ions, the sample is held at 8 kV and both grids are held at ground. Second, for the postionization experiments, a two-step acceleration is used with the sample at 8 kV, the first grid at 7.6 kV, and the second grid at ground. In practice, the extraction potentials in the ion source are adjusted to optimize resolution for the ions formed by photoionization of desorbed neutral molecules. The overall flight path length is 120 cm with acceleration distances of 4 mm for each of the two acceleration regions. The accelerated ions are detected by using a dual-channel plate detector. Data are recorded in a transient recorder with a maximum time resolution of 5 ns. Further processing of the data is accomplished in a PC-based software system. The typical operating vacuum is $\sim 2 \times 10^{-9}$ Torr. The mass resolution $m/\Delta m$ of the apparatus is approximately 1000 (FWHM) with a 5-ns laser pulse, while a <100-psec, 266-nm laser pulse yields a resolution exceeding 1500 with the same apparatus.

B. Fourier-Transform Instrument

The laser-desorption FTMS is shown in Fig. 3, and the basic aspects of FTMS are discussed in detail by Marshall and Verdun.[17] The instrument includes a superconducting solenoid (~7 T), a heatable and coolable sample introduction system, and a 2 in. × 2 in. × 3 in. (5.08 cm × 5.08 cm × 7.62 cm) ion-trapping cell for storing and detecting the laser-desorbed ions. A LiF window provides access for the

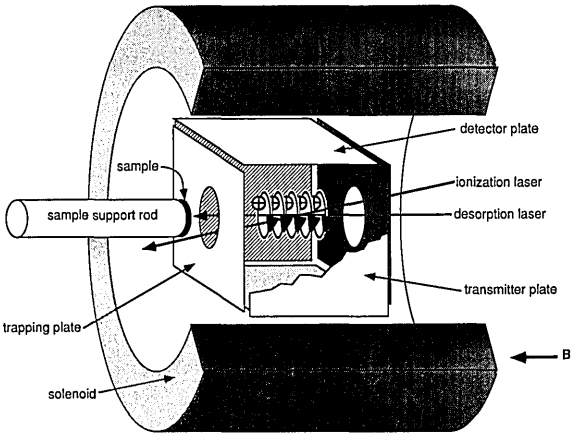

Fig. 3. Laser-desorption FTMS utilized in the current work.

laser beam to desorb ions or neutral molecules from the substrates. Either ions are trapped in the cell directly or neutral molecules are postionized with a second laser inside the cell. The ion cyclotron resonance cell consists of three pairs of opposing, electrically isolated Mo plates. The ions are trapped with the trapping plates set at ~1 V and are then accelerated into larger radii of the cyclotron motion (~1 cm) by using either rf or impulse excitation on the transmitter plates. The coherently excited ion packets induce an image charge on the detector plates that is then converted to a voltage. This voltage is amplified and collected in an analog-to-digital converter in a PC with an analog-to-digital conversion rate of up to 16 MHz; 256-K data points can be acquired for each transient. This signal is transformed into a frequency spectrum by Fourier transformation. The mass spectrum is obtained by using $m = qB/\omega$, where ω is the cyclotron frequency (in radians/second), m/q is the mass/charge ratio for the ion of interest, respectively, and B is the magnetic field. This is accomplished by an Ionspec Omega data collection system. Mass resolutions exceeding 10^5 ($m/\Delta m$) are routinely achieved and a resolution of $>10^6$ (at $m/q = 200$) has been obtained. The number of detected ions varies from $\sim 10^3$ (detection limit) to $\sim 10^6$ (space charge limit).

The sample introduction system consists of a 1½-in.- (3.81-cm-) diameter, highly polished stainless-steel transfer rod with a heatable and coolable sample mount at the end. The rod passes through a vacuum-pumped, double O-ring seal (Cajon connection) into the sample introduction chamber. This sample interchange region is pumped by a 170-L/s turbo molecular pump and has a quick-change 6-in. (15.24-cm) conflat door. The rod then passes through a Teflon differential pumping aperture into the sample preparation region that contains an ion sputtering gun, viewports, and is pumped with a 240-L/s turbo molecular pump. The rod is passed through a second Teflon differential pumping aperture into the third region that contains the FTMS cell (which was described above). This region is pumped with a 1500 L/s cryopump. The operating (with sample next to the FTMS cell) pressures for the separate regions are 10^{-7}, 10^{-8}, and 10^{-9} Torr, respectively. The samples are either placed onto the substrates directly, placed onto the substrate with double-stick adhesive tape, or are evaporated onto the substrates.

C. Laser Facilities

We utilize various lasers for desorption and postionization. Typically the 532-nm focused output (or 266-nm doubled output) of a Q-switched, mode-locked Nd^{3+}:YAG laser (<100-psec pulse duration) is used for desorption. One of a multiple of frequencies generated with a nanosecond-type Nd^{3+}:YAG laser is used for the postionization step. These wavelengths (and energies) include 1064-nm (the fundamental 1.16 eV), 532-nm (second-harmonic 2.33 eV), 355-nm (third-harmonic 3.49 eV), 266-nm (fourth-harmonic 4.66 eV), 212.8-nm (fifth-harmonic 5.83 eV), and 118-nm radiation (ninth-harmonic 10.5 eV), all generated directly from the output of the Nd:YAG laser. We also use a XeCl excimer laser (308 nm, 4 eV) for desorption or for postionization. Also, we have constructed two high-resolution, high-power, tunable dye lasers. These dye lasers are pumped by the 532-nm output of the Nd:YAG laser. The outputs of these lasers have been frequency doubled and tripled in various harmonic-generation crystals (KDP and BBO) to provide tunable radiation across the UV and visible. In addition to these easily generated laser wavelengths, we have recently employed these dye lasers for producing tunable VUV light. This radiation is generated by four-wave mixing in Kr gas (resonant difference–frequency mixing)[18–20] to provide tunable VUV radiation from ~110 to 200 nm (11.3–6.2 eV photons). This tunability permits selective ionization of different species. Another use for this tunable VUV is for gentle photoionization of large molecules. These species have been difficult to photoionize because of fragmentation following photon absorption.[21,22] The observed fragmentation is caused by excess energy deposited in the photoion. It should be possible to tune the photon energy of the photoionization laser to just above the threshold for ionization. This should leave the ion with relatively little excess energy and, thus, small amounts of fragmentation.

The lasers are independently triggered, which permits their relative timing to be adjusted. An iris is used to pick out the central portion of the desorption laser beam, and a series of neutral density filters is used to regulate the beam intensity. The desorption laser is obliquely incident on the sample for the TOF and normally incident for the FTMS. The energy is typically less than 0.01 mJ/pulse, with an irradiated area of $<10^{-3}$ cm^2. The ionization laser intensity can be continuously varied by using a set of mirror-image beam splitters (one high reflector at a specified wavelength, one uncoated) rotated in opposite senses to keep the beam from deviating in position and direction.

3. Results

A. Surface Analysis: Vulcanizates

A number of previous researchers have described experiments relating to polymer mass spectrometry.[23–26] Below we describe our method for detecting additives in polymers. A detailed report on these experiments is forthcoming.[27] Figures 4–6 show three laser-desorption mass spectra obtained from vulcanizate A and B (both of which are commercial rubbers).[28] The front side of a 1-cm^2 2-mm-thick rubber sample was scraped with a razor blade to expose fresh material for molecular analysis. The samples were held in place on the sample stub with a press-fit ring holding a copper foil with a 4-mm-diameter hole cut out of the center. The upper spectrum displayed in Fig. 4 was acquired by using 355-nm postionization. The signal obtained with

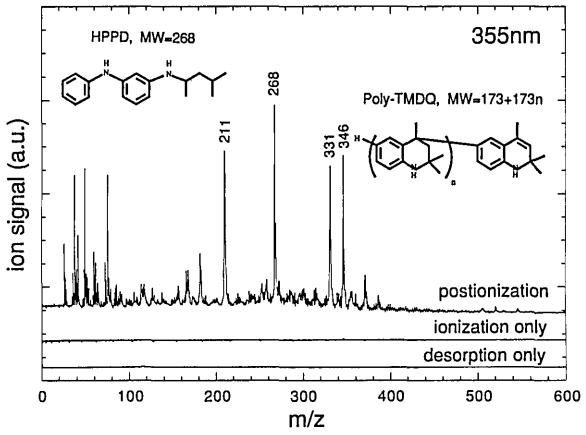

Fig. 4. TOF mass spectra of vulcanizate B. The spectra taken with desorption only (postionization laser blocked) and ionization only (desorption laser blocked) yield a weak signal. The large peaks in the postionization spectrum are indicative of certain additives in this vulcanizate (see text for details). The spectra are offset vertically for clarity.

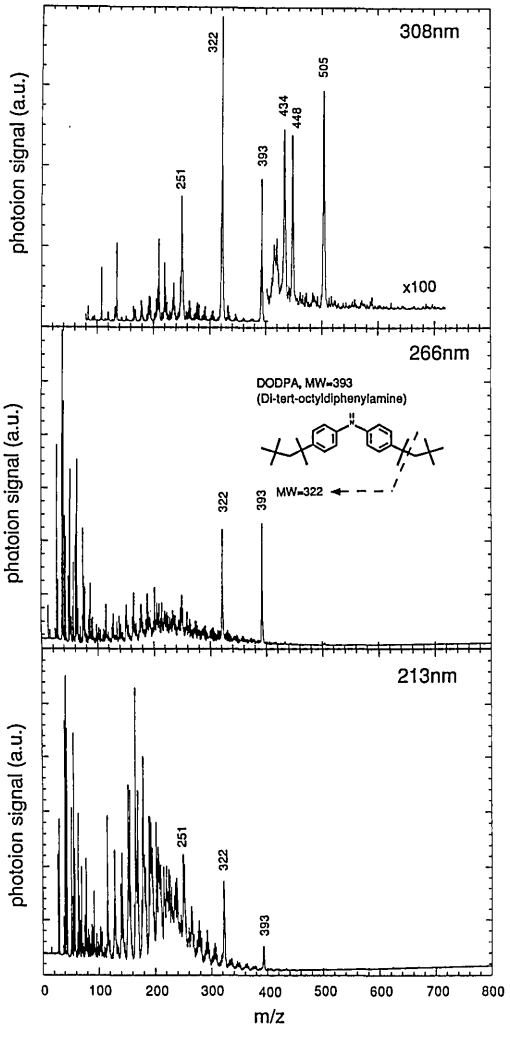

Fig. 5. Postionization of vulcanizate A by the use of 308, 266, and 213-nm radiation for the ionization laser. Compared with the 308-nm postionization data, the 213-nm radiation yields molecular ions that are characteristic of the bulk of the polymer and not just additives.

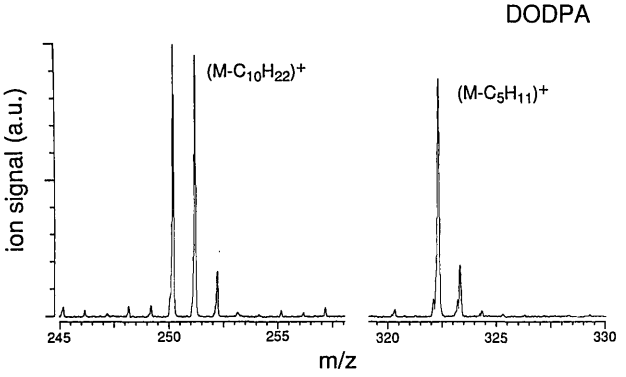

Fig. 6. Fourier-transform mass spectra of postionization of laser-desorbed vulcanizate A showing the two most abundant fragments of DODPA with sufficient resolution for mass determination.

the ionization laser blocked (desorption only) or the desorption laser blocked (ionization only) is also plotted. This shows that we are truly probing the desorbed neutral molecules. As is clearly evident from Fig. 5, different postionization wavelengths produce different mass spectra. Photoionization that uses the longer wavelength (>300 nm) strongly favors the formation of ions that are indicative of additives (Figs. 4 and 5), whereas, with a shorter wavelength, the selectivity for the additives is reduced more and more, and the spectrum is dominated by mass peaks arising from the rubber backbone. The major additive detected in vulcanizate B (Fig. 4) is *N*-(1,3-dimethylbutyl)-*N'*-phenyl-*p*-phenylenediamine (HPPD), an antiozonant, which yields molecular ions at $m/z = 268$ (parent ion), 211 $(M - C_{11}H_9)^+$, 183, and 169. Furthermore, vulcanizate B contains poly-(2,2,4-trimethyl)-1,2-dihydroquinoline (poly-TMDQ), an antioxidant, as is evidenced by $m/z = 346$ (parent M^+) and 331 $(M - CH_3)^+$ in this polymeric mixture. In vulcanizate A (Fig. 5), the major additive is di-tert-octyldiphenylamine (DODPA), also an antioxidant, which forms the photoions $m/z = 393$ (parent M^+), 322 $(M - C_5H_{11})^+$, and 251 $(M - C_{10}H_{22})^+$. A DODPA impurity, tri-tert-octyldiphenylamine, is also detected with the parent at $m/z = 505$ (M^+), and the fragments $m/z = 448$ $(M - C_4H_9)^+$ and 434 $(M - C_5H_{11})$.$^+$

This selectivity permits the study of various additives that are present only at the percent level. Without this selectivity, these additive peaks would be obscured by the many peaks arising from the ionization of the rubber polymer and other additives. Shorter postionization wavelengths (Fig. 5) ionize most of the other larger molecular species that are present in the sample, and can therefore be utilized to obtain a nondiscriminative mass spectrum of the vulcanizate. However, 213-nm radiation does not effectively ionize most of the smaller fragments present because they have higher ionization potentials. Shorter wavelength light (i.e., photon energy above the ionization potential) permits detection of these smaller fragments.[24,27] Figure 6 displays a high-resolution Fourier-transform mass spectrum of the

DODPA fragment m/z = 322 amu and m/z = 251 amu. The ability of absolute mass determination without the use of a standard, together with the high resolution, permits unambiguous identification of the mass peaks as fragments from the DODPA parent molecule.

B. Fullerenes

The discovery of a new class of carbon molecules, termed fullerenes,[29–33] has stimulated intense activity in physical chemistry. Extensive study of the formation of fullerene molecules, solvent extractions, and the synthesis of chemical compounds necessitate high-performance mass characterization at high molecular weights (m/z = 500–5000 amu). Laser-based mass spectrometry proved its utility in the course of these investigations.[34] A typical example of a mixture of fullerenes from a toluene extraction is displayed in Fig. 7(a), which was taken with the FTMS instrument by using laser-desorption and post-ionization.[35–37] The major species identified in the extract are C_{60}, C_{70}, C_{78}, and a few higher-mass fullerenes. The fragment peaks (to the left of the identified mass peaks) arise from photodissociation by the photoionization laser.[15,38] The appearance of only even-numbered fullerenes from photodissociation implies that only C_2 fragments are lost, as has been discussed in detail previously by O'Brien *et al.*[38] Since no signal is observed when either the desorption laser or the postionization laser are blocked, the recorded mass spectrum is indicative of the neutral flux desorbed from the surface. The mass resolution $m/\Delta m$ in the spectrum of Fig. 7(a) is limited to ~2000 because of space charge effects in the cell (i.e., too many ions are present in the cell). By reducing the number of ions in the trapping cell, a higher mass resolution ($m/\Delta m$ ~ 20,000) spectrum is obtained and is shown in Fig. 7(b). This spectrum was obtained by trapping the direct ions in the cell. The different isotopic peaks arise from the 1.1% natural abundance of ^{13}C relative to ^{12}C and are labeled in the figure. We have achieved resolutions in excess of 1,300,000 with laser desorption from certain samples.[39]

To obtain more quantitative information on the abundance of the different fullerene molecules in our samples, we used postionization of the desorbed neutral molecules. Figure 8 shows that single-photon postionization can simplify the interpretation of mass spectrometric results. Multiphoton ionization (355 nm) causes major fragmentation of even these extremely stable molecules. The comparison with single-photon ionization (118 nm) of the same sample provides a much clearer picture of the nature of the fullerene mixture.

One example of a mass spectrometric analysis of a complex mixture of C_{60} reaction products is shown in Fig. 9. These mass spectra were taken of C_{60} refluxed for 20 h in 1,2,3,5-tetramethylbenzene. The top spectrum is a low-resolution laser desorption (266-nm) TOF mass spectrum. The bottom high-resolution laser desorption (532-nm) FTMS spectrum shows the adduct of one solvent molecule with C_{60} at mass 853. Methyl addition and loss are indicated in the multiplets on both sides of the central peaks. In addition, H gain and loss are evident. Clearly, the analysis of these complex fullerene reaction products requires a high-resolution mass spectrometer such as the FTMS.

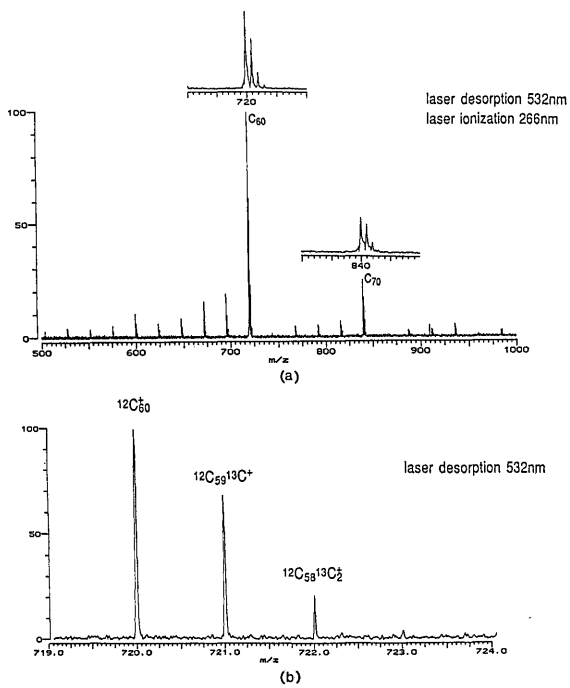

Fig. 7. FTMS spectra acquired with (a) postionization by 266-nm photons and with (b) prompt ion detection.

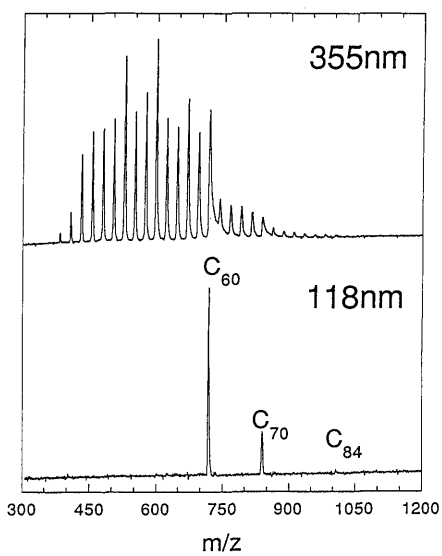

Fig. 8. Laser-desorption–laser-ionization TOF spectra of a toluene extract of fullerene molecules. The top spectrum was obtained by using 355-nm photoionization and displays considerable fragmentation. The bottom spectrum was obtained by using 118-nm radiation and displays the lack of fragmentation from single-photon ionization.

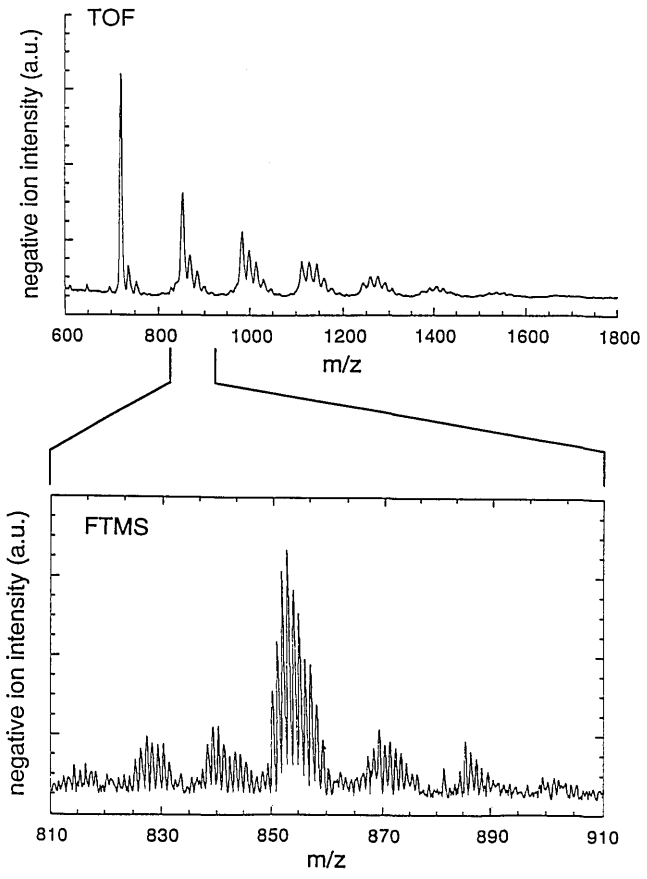

Fig. 9. Reaction products from C_{60} refluxed for 20 h in 1,2,3,5-tetramethylbenzene.

C. Desorption Fundamentals

In order to analyze these samples quantitatively, we have investigated the laser-desorption process itself by measuring the velocity distributions of laser-desorbed neutral C_{60} and C_{70} molecules. The velocity distributions are determined by permitting the desorbed neutral species to travel a defined short distance before ionization and acceleration into the mass spectrometer occurs. By varying the time delay between desorption and ionization, the velocity distribution is obtained. Figure 10 shows the distribution for C_{60} with a Maxwellian fit to 2070 K. Good agreement of the experimental data with a Maxwellian distribution is found. We conclude that, at the applied laser fluences, C_{60} molecules are desorbed by evaporation that is induced by the incident radiation, providing no fragmentation in the desorption process.

We have also measured the threshold fluence for laser desorption of neutral and ionic C_{60} (Fig. 11). The threshold for neutral C_{60} is almost an order of magnitude lower than the threshold for positive-ion production. This seems to be a feature that most solid materials have in common: desorption thresholds for neutral production are significantly lower than for ion production. This gives the postionization technique a large advantage over the prompt ion detection techniques used in the past. The ability to

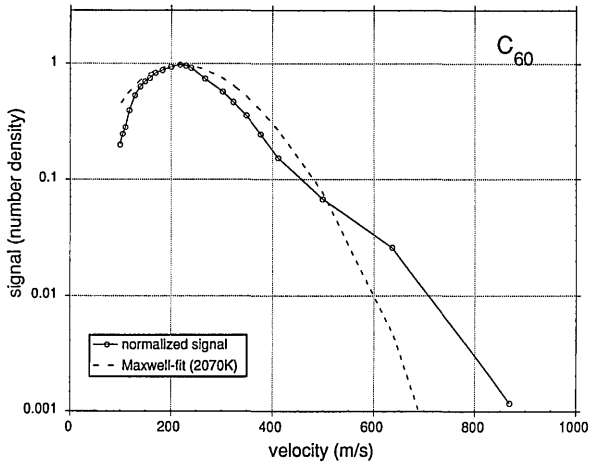

Fig. 10. Velocity distribution for C_{60} laser desorbed from a stainless-steel sample probe. The dashed curve is a best fit to a Maxwellian distribution.

optimize the desorption laser (wavelength, photon fluence, pulse length) and the ionization laser separately offers the possibility of realizing fragmentation-free desorption and ionization. Once this is achieved, the capability of quantitative molecular surface analysis exists.

D. Multiphoton versus Single-Photon Ionization of Large Molecules

Because of the many vibrational degrees of freedom for a large molecule ($3n - 6$, where n is the number of atoms in the molecule), the density of vibrational states, even at moderate excitations (near-UV-visible photon excitation), is enormous. Thus the rate of conversion of internal energy will be high (i.e., internal electronic-to-vibrational transfer will occur on extremely short time scales). Therefore more laser photons will be required for ionizing a large molecule than the mere ionization potential would suggest. The molecular ion thus produced is left with large

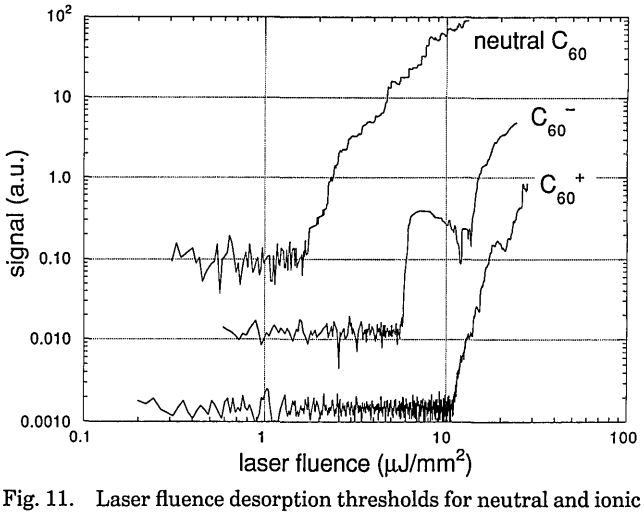

Fig. 11. Laser fluence desorption thresholds for neutral and ionic molecules from a C_{60} sample. The curves are vertically offset for clarity.

amounts of internal excitation, which is referred to below as a superexcited molecule. In this case, multiphoton ionization is a competition between electronic excitation that is due to photon excitation and excitation loss into vibrational energy levels. An additional important loss channel is present: fragmentation. Thus the fraction of molecules ionized depends not only on absorption cross sections and internal conversion rates but also on the stability of the molecule in question. C_{60} is a good molecule for this study because of its symmetry and stability. In fact, we have evidence that C_{60} can accumulate >60 eV/molecule before dissociating.[40] The major pathways for energy loss from this photoexcited species include direct photoionization, fragmentation, photon emission, delayed ionization (thermionic), and fragmentation followed by photoionization during the 10-ns laser pulse. These types of energy-loss phenomena also exist in macroscopic species, such as thin films and systems in which heat transport is negligible. The observed processes, although studied only for C_{60} so far, should always occur for sufficiently large molecules during multiphoton ionization.

In a separate experiment, we studied the fate of superexcited molecules. These experiments were performed in the TOF mass spectrometer and are discussed in detail in a forthcoming article.[40] We have detected, proved, and theoretically modeled delayed ionization of C_{60}. Careful observation of the postionization TOF mass spectra of C_{60} shows that the parent mass peak is asymmetric (tailed) toward longer flight times (see Fig. 8, top spectrum). Furthermore these tails exhibit the same dependence on laser fluence as the fragmentation of C_{60}. The tails are attributed to thermionic emission of electrons from C_{60} molecules following multiphoton absorption. Additional evidence for the observation of thermionic emission is the detection of the arrival time of the photoelectrons. We find identical tails for photoions and photoelectrons. Fragmentation-free ionization without any delayed emission is observed only for single-photon ionization wavelengths at all accessible laser fluences. The absence of thermionic emission at 118 nm permits maximum mass resolution that enables us to resolve the isotope pattern of C_{60} ($m/\Delta m > 1500$).

The destruction of photoexcited C_{60}^+ has been postulated to occur by means of a sequential loss of C_2 units.[38] In an effort to further characterize the fragmentation behavior of C_{60}, we have recently detected C atoms from the multiphoton dissociation of laser-desorbed C_{60}. The (2 + 1) resonantly enhanced multiphoton ionization (REMPI) spectrum of C atoms[41,42] is shown in Fig. 12. The REMPI detection laser is also the dissociation laser. The dissociation intensity is ~ 1 GW/cm^2, which is far above the dissociation threshold.[40] Since the dissociation laser may also crack the fragments from C_{60}, we cannot conclude that C atoms come directly (in one step) from the dissociation of the parent molecule. They

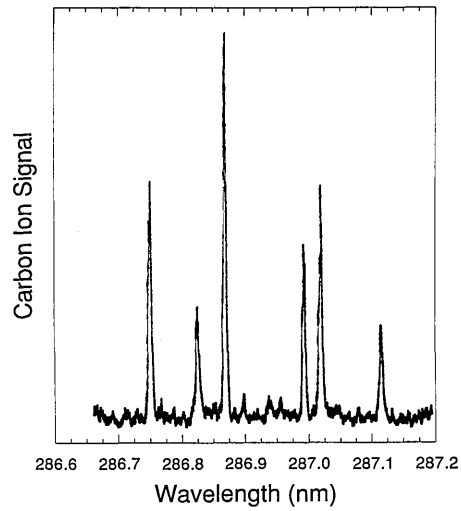

Fig. 12. (2 + 1) REMPI spectrum of C atoms from the dissociation of C_{60} at ~ 287 nm. The two-photon resonant transition is $^3D \leftarrow {}^3P$ and the third photon ionizes the excited C atom.

may indeed appear from the dissociation of C_2 or a larger fragment. To prove that C_{60} does dissociate into C atoms or C_2 units, a single-photon resonant transition for detecting either C or C_2 is required. We are currently studying C_2 neutrals with laser-induced fluorescence and C atoms with (1 + 1) REMPI, using a tunable VUV laser for the first (resonant) transition.

E. Tunable VUV

In an effort to achieve fragmentation-free photoionization of desorbed molecules (avoiding the above-mentioned processes by tuning the photon energy to just above the ionization limit of the molecule of choice), we have recently set up a tunable VUV laser system. These photons are generated by four-wave mixing in Kr gas and by utilizing a two-photon resonance in Kr to accentuate the difference frequency. Figure 13 shows our setup for generating

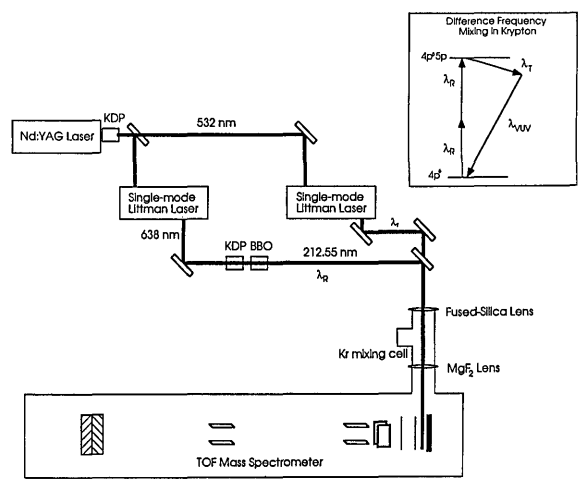

Fig. 13. Setup for the tunable vacuum ultraviolet laser/time-of-flight mass spectrometer. The difference frequency mixing scheme is depicted in the inset.

the VUV light and transporting it to the ionization region of the TOF mass spectrometer. The typical outputs from the dye lasers are 50 mJ/pulse for the 638-nm Littman laser (after three stages of amplification) and 10 mJ/pulse for the tunable laser (after one stage of amplification). The beams are then telescoped to achieve reasonably well-matched focal parameters before they are combined on a dichroic beam splitter. The overlap, and thus the VUV intensity, can be optimized by observing a mass spectrum for acetone, methanol, or some other molecule with a low ionization potential. In addition to the two-photon transition of Kr at 212.55 nm, we have employed the transition at 216.7 nm for the resonant-enhanced two-photon step. In practice, the Kr is added to some pressure (usually ~10–100 Torr), the ionization signal is optimized, and then the Kr pressure is optimized. For certain VUV wavelength ranges, another rare gas (Xe or Ar) may be added to the Kr to achieve phase-matched conditions.

Figure 14 displays a 50-cm^{-1} scan through a (so far) unknown autoionizing resonance in Au near the ionization threshold. The resonant two-photon transition involved is at 216.7 nm (92308.177 $cm^{-1}/2$). For this work, a Au foil was placed over the stainless-steel sample holder. The desorption laser was the *Q*-switched, mode-locked frequency-doubled Nd:YAG laser at 532 nm and a 20-Hz repetition rate. A photoionization spectrum for toluene was obtained simultaneously to ensure constant VUV intensity. The linewidth of this feature yields a lower limit for the lifetime of the autoionizing state of 1.4 ps. Since we are using this autoionization feature in Au as a demonstration of the technique of laser desorption/VUV postionization, we have not pursued the spectral analysis of this feature.[43,44]

Figure 15 shows a laser-desorption tunable VUV photoionization mass spectrum of C_{60} and C_{70} by using 127.53 nm. The fullerene peaks show no delayed ionization and no fragmentation (see Ref. 40 for a detailed explanation of these phenomena). Additionally, although the actual number of VUV photons/pulse has not been measured, the signal-to-noise ratio implies that there is more photoionization signal in this spectrum than in the 118-nm C_{60} spectrum shown in Fig. 8.

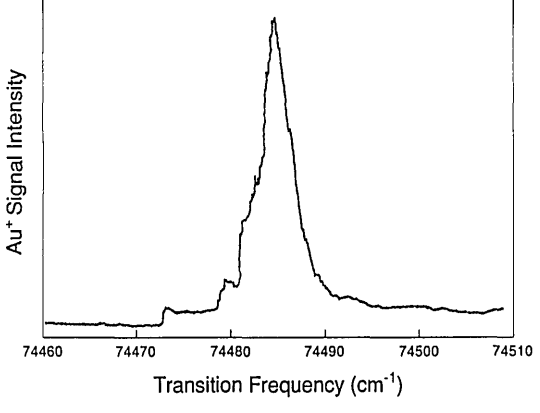

Fig. 14. VUV laser scan at ~9.2 eV. Some of the fluctuations may be from shot-to-shot reproducibility problems inherent in the laser-desorption process.

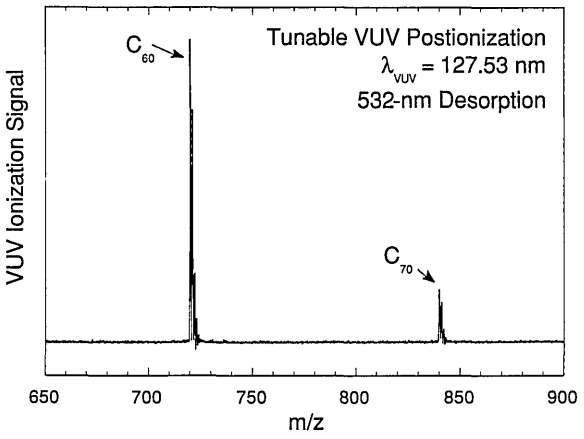

Fig. 15. VUV photoionization mass spectrum of C_{60} and C_{70}.

4. Conclusions

Laser desorption/postionization has been applied to surface analytical work and can display either a species-specific detection (resonantly enhanced multiphoton ionization) or a nonspecific detection. By exercising both of these options, complicated mixtures have been analyzed for surface species. Laser desorption followed by laser ionization has been used to study different additives in a variety of rubbers (vulcanizates). Different wavelengths for the postionization laser selectively ionize certain additives in the polymers. VUV light nonselectively ionizes the species that have been laser desorbed from the polymer. The coupling of high-resolution TOF and FTMS's to selective postionization wavelengths permits a specificity in detecting additives in polymers. Diffusion and segregation phenomena will be studied by using these techniques in the future.

Other workers in the field of laser-desorption mass spectrometry[45,46] have used laser desorption followed by cooling of the desorbed species in a pulsed supersonic jet. We forego the additional inconvenience of a pulsed jet and, instead, postionize the desorbed neutrals within ~1 mm of the surface. In addition to ease of use, the present setup permits increased sensitivity and the ability to collect direct (prompt) desorbed ions as well as postionized neutral molecules. In fact, the present setup allows for ~1–10% efficiency in the ionization of the desorbed plume, whereas the supersonic jet scheme allows for only ~10^{-5} efficiency in ionization of the desorbed plume.

Laser desorption, followed by laser ionization, has been used to study the photophysics of C_{60} and related fullerenes. Since C_{60} has become available in macroscopic quantities, numerous interesting properties that are important for the molecular mass spectrometry community have been observed and documented. These studies have been greatly accelerated and, in

some cases, made possible only through the use of high-resolution laser-desorption mass spectrometry. The continued study of fullerenes and related compounds will yield new and unique results in chemical physics and materials science.

We thank R. P. Lattimer and D. M. Gruen for many useful discussions. This work was supported by the U.S. Department of Energy, BES-Materials Sciences, under contract W-31-109-ENG-38.

References

1. L. C. Feldman and J. W. Mayer, *Fundamentals of Surface and Thin Film Analysis* (North Holland, New York, 1986).
2. M. E. Brubaker and M. Trenary, "Adsorbate ordering processes and infrared spectroscopy: an FT-IRAS study of N_2 chemisorbed on the Ni (110) surface," J. Chem. Phys. **85,** 6100–6109 (1986).
3. Erley, "Reflection-absorption infrared spectroscopy of adsorbates on a Cu (111) single crystal surface," J. Electron Spectrosc. Relat. Phenom. **44,** 65–78 (1987).
4. Y. R. Shen, "Optical second harmonic generation at interfaces," Ann. Rev. Phys. Chem. **40,** 327–350 (1989).
5. A. L. Harris, C. E. D. Chidsey, N. J. Levinos, and D. N. Loiacono, "Monolayer vibrational spectroscopy by infrared-visible sum generation at metal and semiconductor surfaces," Chem. Phys. Lett. **141,** 350–356 (1987).
6. R. W. Odorn and B. Schueler, "Thin film microanalysis using laser ablation and laser ionization mass spectrometry," Thin Solid Films **154,** 1–10 (1987).
7. L. J. Kovalenko, C. R. Maechling, S. J. Clemett, J.-M. Philippoz, R. N. Zare, and C. M. O. Alexander, "Microscopic organic analysis using two-step laser mass spectrometry: application to meteoritic acid residues," Anal. Chem. **64,** 682–690 (1992).
8. M. S. de Vries, D. J. Elloway, H. R. Wendt, and H. E. Hunziker, "Photoionization mass spectrometer with a microscope laser desorption source," Rev. Sci. Instrum. **63,** 3321–3325 (1992).
9. J. F. Ready, *Effects of High-Power Laser Radiation,* (Academic, New York, 1971).
10. *Lasers and Mass Spectrometry,* D. M. Lubman, ed. (Oxford U. Press, New York, 1990).
11. R. Srinivasan, B. Braren, R. W. Dreyfus, L. Hadel and D. E. Seeger, "Mechanism of the UV laser ablation of polymethyl methacrylate at 193 and 248 nm: laser-induced fluorescence analysis, chemical analysis, and doping studies," J. Opt. Soc. Am. B. **3,** 785–791 (1986).
12. Y. Li, R. T. McIver, and J. C. Hemminger, "Experimental determination of thermal and nonthermal mechanisms for laser desorption from thin metal films," J. Chem. Phys. **93,** 4719–4723 (1990).
13. S. Lazare and V. Granier, "Ultraviolet laser photoablation of polymers: a review and recent results," Laser Chem. **10,** 25–40 (1989).
14. R. Srinivasan and B. Braren, "Ultraviolet laser ablation of organic polymers," Chem. Rev. **89,** 1303–1316 (1989).
15. P. Wurz, K. R. Lykke, M. J. Pellin, and D. M. Gruen, "Velocity distributions and photodissociation of C_{60} and C_{70}," J. Appl. Phys. **70,** 6647–6652 (1991).
16. J. E. Hunt, K. R. Lykke, and M. J. Pellin, "Laser desorption/photoionization time-of-flight mass spectrometry of polymer additives," in *Methods and Mechanisms for Producing Ions from Large Molecules* (Plenum, Minaki, Canada, 1990), pp. 309–314.
17. A. G. Marshall and F. R. Verdun, *Fourier Transforms in NMR, Optical, and Mass Spectrometry* (Elsevier Science, Amsterdam, 1990).
18. R. Hilbig and R. Wallenstein, "Tunable VUV radiation generated by two-photon resonant frequency mixing in xenon," IEEE J. Quantum Electron. **QE-19,** 194–201 (1983).
19. C. Y. Ng, *Vacuum Ultraviolet Photoionization and Photodissociation of Molecules and Clusters* (World Scientific, Singapore, 1991), p. 572.
20. J. P. Marangos, N. Shen, H. Ma, M. H. R. Hutchinson, and J. P. Connerade, "Broadly tunable vacuum-ultraviolet radiation source employing resonant enhanced sum-difference frequency mixing in krypton," J. Opt. Soc. Am. B **7,** 1254–1259 (1990).
21. R. J. J. M. Steenvoorden, P. G. Kistemaker, A. E. de Vries, L. Michalak, and N. M. M. Nibbering, "Laser single photon ionization mass spectrometry of linear, branched and cyclic hexanes," Int. J. Mass Spectrom. Ion Processes **107,** 475–489 (1991).
22. S. E. Van Bremer and M. V. Johnston, "10.5 eV photoionization mass spectrometry of aliphatic compounds," J. Am. Soc. Mass Spectrom. **1,** 419–426 (1990).
23. R. Larciprete and M. Stuke, "Direct observation of excimer-laser photoablation from polymers by picosecond-UV-laser mass spectroscopy," Appl. Phys. B **42,** 181–184 (1987).
24. J. B. Pallix, U. Schüle, C. H. Becker, and D. L. Huestis, "Advantages of single-photon ionization over multiphoton ionization for mass spectrometric surface analysis of bulk organic polymers," Anal. Chem. **61,** 805–811 (1989).
25. T. Imasaka, K. Tashiro, and N. Ishibashi, "Supersonic jet spectrometry of chemical species laser ablated from organic polymers," Anal. Chem. **61,** 1530–1533 (1989).
26. D. A. Lustig and D. M. Lubman, "Selective resonance enhanced multiphoton ionization of aromatic polymers in supersonic beam mass spectrometry," Int. J. Mass Spectrom. Ion Processes **107,** 265–280 (1991).
27. K. R. Lykke, D. H. Parker, P. Wurz, J. E. Hunt, M. J. Pellin, D. M. Gruen, J. C. Hemminger, and R. P. Lattimer, "Mass spectrometric analysis of rubber vulcanizates by laser desorption/laser ionization," Anal. Chem. **64** (to be published).
28. R. P. Lattimer, R. E. Harris, and C. K. Rhee, "Identification of organic additives in rubber vulcanizates using mass spectrometry," Anal. Chem. **58,** 3188–3195 (1986).
29. E. A. Rohlfing, D. M. Cox, and A. Kaldor, "Production and characterization of supersonic carbon cluster beams," J. Chem. Phys. **81,** 3322–3330 (1984).
30. H. W. Kroto, J. R. Heath, S. C. O'Brien, R. F. Curl, and R. E. Smalley, "C_{60}: Buckminsterfullerene," Nature (London) **318,** 162–163 (1985).
31. W. Kratschmer, L. D. Lamb, K. Fostiropoulos, and D. R. Huffman, "Solid C_{60}: a new form of carbon," Nature (London) **347,** 354–358 (1990).
32. R. E. Smalley, "Supersonic carbon cluster beams," in *Atomic and Molecular Clusters,* E. R. Bernstein, ed. (Elsevier, New York, 1990), pp. 1–68.
33. R. Taylor, J. P. Hare, A. K. Abdul-Sada, and H. W. Kroto, "Isolation, separation and characterization of the fullerenes C_{60} and C_{70}: the third form of carbon," J. Chem. Soc. Chem. Commun. **1990,** 1423–1425 (1990).
34. D. H. Parker, K. Chatterjee, P. Wurz, K. R. Lykke, M. J. Pellin, L. M. Stock, and J. C. Hemminger, "Fullerenes and giant fullerenes: synthesis, separation, and mass spectrometric characterization," Carbon (to be published).
35. K. R. Lykke, M. J. Pellin, P. Wurz, D. M. Gruen, J. E. Hunt, and M. R. Wasielewski, "Spectrometric characterization of purified C_{60} and C_{70}," in *Materials Research Society Symposium Proceedings,* R. S. Averback, J. Bernholc, and D. L. Nelson, eds. (Materials Research Society, Boston, Mass., 1990), Vol. 206, pp. 679–686.
36. D. H. Parker, P. Wurz, K. Chatterjee, K. R. Lykke, J. E. Hunt, M. J. Pellin, J. C. Hemminger, D. M. Gruen, and L. Stock,

"High yield synthesis, extraction and mass spectrometric characterization of fullerenes C_{60} to C_{266}," J. Am. Chem. Soc. **113,** 7499–7503 (1991).
37. G. Meijer and D. S. Bethune, "Mass spectrometric confirmation of the presence of C_{60} in laboratory-produced carbon dust," Chem. Phys. Lett. **175,** 1–2 (1990).
38. S. C. O'Brien, J. R. Heath, R. F. Curl, and R. E. Smalley, "Photophysics of buckminsterfullerene and other carbon cluster ions." J. Chem. Phys. **88,** 220–230 (1988).
39. M. J. Pellin, K. R. Lykke, P. Wurz, and D. H. Parker, "Molecular surface analysis by laser ionization of desorbed molecules," Am. Inst. Phys. Conf. Ser. (to be published).
40. P. Wurz and K. R. Lykke, "Multiphoton excitation, dissociation and ionization of C_{60}," J. Phys. Chem. (to be published).
41. L. J. Moore, J. D. Fassett, J. C. Travis, T. B. Lucatorto, and C. W. Clark, "Resonance-ionization mass spectrometry of carbon," J. Opt. Soc. Am. B **2,** 1561–1565 (1985).
42. S. T. Pratt, J. L. Dehmer, and P. M. Dehmer, "Photoelectron angular distributions from resonant multiphoton ionization of atomic carbon," J. Chem. Phys. **82,** 676–680 (1985).
43. E. Jannitti, A. M. Cantu, T. Grisendi, M. Pettini, and G. P. Tozzi, "Absorption spectrum of AuI in the vacuum ultraviolet," Phys. Scr. **20,** 156–162 (1979).
44. U. Kronert, S. Becker, T. Hilberath, H.-J. Kluge, and C. Schulz, "Resonance ionization mass spectroscopy with a pulsed thermal atomic beam," Appl. Phys. A **44,** 339–345 (1987).
45. G. Meijer, M S. de Vries, H. E. Hunziker, and H. R. Wendt, "Laser desorption jet-cooling spectroscopy of para-amino benzoic acid monomer, dimer, and clusters," J. Chem. Phys. **92,** 7625–7635 (1990).
46. J. Grotemeyer, U. Boesl, K. Walther, and E. W. Schlag, "A general soft ionization method for mass spectrometry: resonance-enhanced multi-photon ionization of biomolecules," Org. Mass Spectrom. **21,** 645–653 (1986).